

# Corrosion rate of copper canisters used for final disposal of nuclear waste, in synthetic ground water and bentonite clay pore water

Jari Aromaa\*, Muhammad Kamran Khalid, Arif Tirto Aji and Mari Lundström

School of Chemical Engineering, Aalto University, P.O. Box 16200, 00075 Aalto, Espoo, Finland.

## ABSTRACT

In this paper we study the corrosion of copper canisters used for final disposal of nuclear waste, in synthetic ground water and bentonite clay pore water. Both waters were studied when in equilibrium either with air or low oxygen atmosphere. The purpose of the research was to study the effect of air-formed oxide films on the general corrosion of copper. The samples were oxidized in air at a maximum temperature of 100°C and maximum time of seven days. Corrosion was studied using long-term weight loss tests up to 20 months, polarization resistance monitoring (LPR) for up to 5 weeks, and quartz crystal microbalance (QCM) for up to 5 days. In the weight loss tests corrosion rates were highest in air-purged ground water, 6-8  $\mu\text{m}/\text{year}$ , and lowest in nitrogen-purged pore water, less than one  $\mu\text{m}/\text{year}$ . In polarization resistance tests the corrosion rates were 2-4  $\mu\text{m}/\text{year}$  in air-purged ground water, and less than one  $\mu\text{m}/\text{year}$  in air-purged pore water. Nitrogen-purging resulted in higher corrosion rates than air-purging indicating that oxygen is not the only oxidant affecting the system and that concentration of dissolved oxygen can also affect passivation. The QCM tests in ground water showed high corrosion rates in the order of 10  $\mu\text{m}/\text{year}$  or more, but in pore water from less than one  $\mu\text{m}/\text{year}$  to 2  $\mu\text{m}/\text{year}$ . The oxide films showed a slight protective effect that decreased with time in ground water but improved

in pore water. In both waters the corrosion rate of oxidized samples was initially 75% of the non-oxidized ones. During the immersion the corrosion rate of oxidized samples increased to 90% in ground waters but decreased to 30-60% in pore waters when compared to non-oxidized samples. Because of the small corrosion rates the experimental errors are large, and the protective effect cannot be estimated with certainty. On the other hand, the possible effect of oxide films to increase corrosion rate can be excluded.

**KEYWORDS:** copper, corrosion, canister, nuclear waste, lifetime prediction.

## INTRODUCTION

The Finnish plan for final disposal of nuclear waste is based on the KBS-3 concept. The spent fuel is encapsulated in gas-tight, corrosion-resistant and load-bearing canisters. The spent fuel assemblies are loaded in cast iron load-bearing inserts, and these inserts are placed into copper canisters. The canisters are disposed in crystalline bedrock at a depth sufficient to isolate the encapsulated spent fuel from the surface environment, about 400 to 700 metres deep. In the deposition holes the canisters are surrounded by a compacted bentonite clay buffer that prevents the flow of water and protects them. Finally, the cavities in the rock that are required for the deposition of canisters are backfilled and closed. The goal of the long-term containment is that the safety functions shall effectively prevent release of disposed radioactive materials into the bedrock

---

\*Corresponding author: jari.aromaa@aalto.fi

for at least several thousands of years. The canister construction and multi-barrier principle are shown in Figure 1 [1, 2].

In this work we studied the corrosion of copper canister material in simulated ground water and bentonite clay pore water using long-term immersion tests, electrochemical monitoring, and Quartz Crystal Microbalance. Our study focuses on the effect of air-developed oxide film on general corrosion. The manufacture of copper canister causes oxidation of copper surface. After assembly the loaded spent fuel will cause increase in canister temperature. The surface temperature is less than 50°C in freely circulating air, but close to 100°C when in a

radiation shield or in the deposition hole with unsaturated bentonite buffer and air space between canister and buffer [3, 4]. Before and after assembly the canisters are stored indoors before transport to underground temporary storage. The time from loading the spent fuel and canister assembly to deposition can be up to a few months and most of it is in underground storage [3, 5]. The thickness of the oxide layer before deposition has been estimated as few tens or few hundreds of nanometres [4].

The oxidation proceeds by oxidation of copper to reddish cuprous oxide  $\text{Cu}_2\text{O}$  followed by oxidation of  $\text{Cu}_2\text{O}$  to cupric oxide  $\text{CuO}$ . The present knowledge of copper oxidation in dry air indicates that the

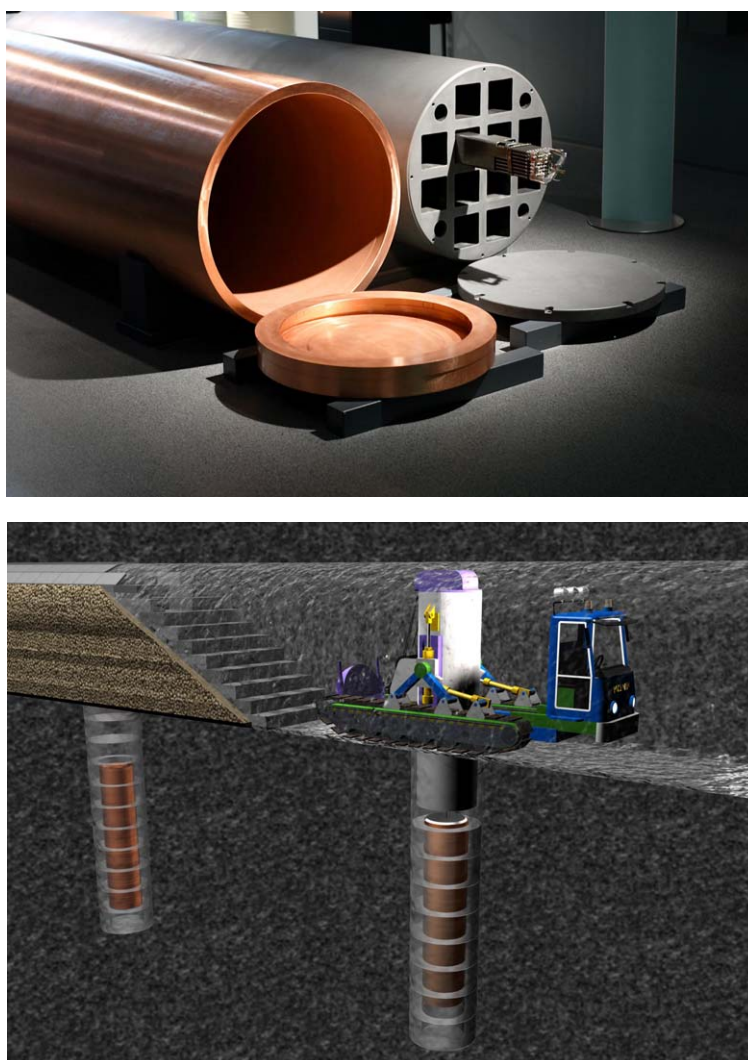


**Figure 1.** The storage canister and multi-barrier principle. Source: Posiva ([www.posiva.fi](http://www.posiva.fi)).

growth follows logarithmic or parabolic rate law, the growth rate decreases with time, and some maximum thickness range is expected. The oxidation kinetics has been found to follow parabolic rate law for example at temperature intervals 50-150°C [6], 80-260°C [7], 110-125°C [8] and 120°C-150°C [9], which suggests a diffusion-controlling oxidation mechanism through the oxide film. At ambient temperature the Cu<sub>2</sub>O growth has been reported to follow inverse logarithmic law [10]. Logarithmic rate law has been reported at 25°C up to 10<sup>6</sup> seconds and Cu<sub>2</sub>O conversion to CuO with time [11]. Logarithmic rate law has been reported when oxide film is growing naturally and deviation from logarithmic law happened when CuO started to form on top of Cu<sub>2</sub>O [12]. Logarithmic law has also been found at 75°C and 100°C [13] and at 30°C and 45°C [14], and a power law at 60°C to 90°C [14]. The oxidation kinetics of Cu to Cu<sub>2</sub>O has also been reported to follow linear rate law, indicating surface reaction controlled oxidation at T = 100-300°C [15] and at 125°C [16]. At ambient temperature the oxide thickness reached 4 nm in five days and 5-6 nm after tens of days and most of the oxide was Cu<sub>2</sub>O [10]. At 140°C and 150°C the oxide film reached thickness of 30 nm in tens of minutes, in an hour at 130°C and in a few hours at 120°C [9]. The CuO phase has been reported to form only at higher temperatures [15]. The oxide film starts to grow as islands and later they coalesce. The growth rate as well as cracking of the oxide film depend on the impurities of copper [6, 17], and impurities in air have resulted in 3 to 8 times thicker oxides [6].

During the installation the buffer and backfill around the canister are not saturated with water. The canisters will be exposed to two different unsaturated environmental conditions. In the encapsulation plant and underground facility, the canisters may be subject to atmospheric corrosion if the relative humidity is sufficiently high. After emplacement of the canisters there will be a period of unsaturated conditions in the compacted bentonite, until the near-field environment (a few meters from the canister) saturates with incoming ground water. The corrosive environment around the canister will be a combination of initial bentonite pore water and saturating ground water. The initial oxygen-containing environment will turn to anoxic as the remaining oxygen is consumed in the corrosion

reactions. The evolution of the near-field environment from the warm and aerobic initial condition to cool and anoxic will change corrosion from relatively rapid and possibly localized to slow and more uniform [4]. In general, corrosion rate has been from less than 1 µm/year [18] to 10-20 µm/year [19] depending on test environment, test type and length. Based on simulations, the corrosion rate will decrease rapidly from the 10 µm/year level to couple of µm/year and after ten or tens of years become zero as all oxidants have been consumed [20]. The realistic estimates for 10<sup>6</sup> years referred in [4] are 0.35 mm for general corrosion and 6 mm for localized corrosion, and maximum estimates are 4 mm for general and 16 mm for localized corrosion.

The air-formed oxide film can affect corrosion in a similar way as the oxide films formed during corrosion consisting of CuO and Cu<sub>2</sub>O. Oxygen reduction on copper is inhibited by metal oxidation into the Cu/Cu<sub>2</sub>O/CuO duplex layer potential region [21]. The oxidation of Cu<sub>2</sub>O by oxygen to CuO can inhibit oxygen reduction. On the other hand, Cu<sub>2</sub>O can increase the total cathodic reaction rate by its own reduction and this could result in slightly faster corrosion [22]. Based on the mixed potential theory, if the rate of oxygen reduction reaction (1)



increases, then the consumption of electrons will increase and that will increase copper corrosion rate. On the other hand, reaction of cuprous chloride species with oxygen can result in cupric ions and they can also act as oxidants [23].

Copper corrosion can be described by direct metal oxidation (2)



In chloride-containing solutions chloride complexes are formed and the reaction mechanism is dependent on potential [24]. At potentials approximately -0.2 V vs. SCE apparent Tafel behaviour is seen, and mixed charge transfer and mass transport controlling kinetics are usually assumed, reaction (3)



At higher potentials close to 0 V vs. SCE film formation happens leading to passivation with a

maximum peak current density and subsequent film or metal dissolution giving a passive range with low current density, reactions (4) and (5).



At potentials close to 0 V vs. SCE and above formation of Cu(II) species can happen, reactions (6) and (7)



$\text{CuCl}_2^-$  is believed to be the main cuprous complex in solutions containing approximately  $0.55 \text{ mol dm}^{-3}$ , like ocean seawater. The anodic dissolution of copper is affected by the movement of  $\text{CuCl}_2^-$  from the copper surface to the bulk electrolyte. The  $\text{CuCl}_2^-$  can be converted into cuprous oxide  $\text{Cu}_2\text{O}$ , reaction (8)



$\text{Cu}_2\text{O}$  is then oxidized to cupric oxide  $\text{CuO}$ . Depending on the solution composition other compounds can form, like atacamite  $\text{Cu}_2(\text{OH})_3\text{Cl}$  in the presence of chloride ions. If the water contains little  $\text{Cl}^-$  but is in carbonate equilibrium with the atmosphere, basic copper carbonate malachite ( $\text{Cu}_2\text{CO}_3(\text{OH})_2$ ) will form. If both  $\text{Cl}^-$  and carbonate species are lacking, tenorite ( $\text{CuO}$ ) is produced. In water with sulfides corrosion products could be cuprous oxide,  $\text{Cu}_2\text{O}$  and brochantite  $\text{CuSO}_4 \cdot 3\text{Cu}(\text{OH})_2 \cdot \text{H}_2\text{O}$  [25].

## MATERIALS AND METHODS

The test material is Cu-OF oxygen-free copper. The copper is described for example in standard SFS-EN 12165 'Copper and copper alloys. Wrought and unwrought forging stock'. The European code is CW008a and UNS number C10200. The minimum copper level is 99.95% including Ag up to maximum 0.015%. Bismuth and lead levels are typical for grade A copper cathodes, 0.0005% and 0.005% respectively. The oxygen content shall be so low that the material conforms to the hydrogen embrittlement requirements of EN 1976, typically max. 10 ppm. The copper canister construction material is same, but some 40-60 ppm phosphorus is alloyed. This should not to our knowledge affect oxidation or corrosion behaviour. For the immersion

tests the samples were 30 mm x 30 mm cut from a 1 mm thick plate. A  $d = 3 \text{ mm}$  hole was drilled in one corner to hang the sample. The sample weight was about 8 grams. For electrochemical tests the samples were cut from 5 mm thick plate and mounted in epoxy. In electrochemical tests an Autolab 31 potentiostat (Metrohm Autolab B.V., Utrecht, The Netherlands) with Nova 2.1 software (Metrohm Autolab B.V., Utrecht, The Netherlands) was used. For the Quartz Crystal Microbalance tests copper was electrochemically deposited on Cr/Au quartz crystals. The electrolyte contained  $75 \text{ g dm}^{-3} \text{ CuSO}_4 \cdot 5\text{H}_2\text{O}$ ,  $190 \text{ g dm}^{-3} \text{ H}_2\text{SO}_4$  and 60 ppm  $\text{Cl}^-$  added as HCl. The deposition current density was  $-5 \text{ mA cm}^{-2}$  and deposition time was 15 minutes resulting in  $1.6 \text{ }\mu\text{m}$  thick deposit. The tests were done using a Stanford Research System SRS QCM200 microbalance (Stanford Research Systems, Sunnyvale, CA, USA).

Before the experiments all the samples were first degreased by ethanol and then immersed in 10 wt-% citric acid for 3 minutes at room temperature. Immersion was repeated 3 times and after each immersion the sample was rinsed with Millipore water and after last immersion with water and ethanol and finally dried. The oxidation of the samples was done in a drying oven (Pol-Eko SLW 53 Smart, Pol-Eko Aparatura, Wodzisław Śląski, Poland). Oxidation treatments were carried out for 3 days at  $60^\circ\text{C}$  and 7 days at  $100^\circ\text{C}$ .

The long-term interval corrosion tests were done in covered 50-litre plastic vessels with gas purging of  $0.25 \text{ dm}^3 \text{ min}^{-1}$ . The experiments were set with interval times of 10 months and 2 months. The principle of the immersion periods is shown in Figure 2. The first three sample sets are introduced when the experiment starts. In the corrosion tests one sample set is taken out after the first interval period, second after two periods and third after four periods. The last sample set is introduced after three periods and removed when the test ends; also it will be in the test for one period. The planned intervals can indicate whether the corrosion rate changes with time (sets A1, A2 and A4) and whether the corrosivity of the test environment changes (sets A1 and B). The tests in this paper are done with lengths of 2, 4, 8, 10, and 20 months.

The polarization resistance tests were done using solid copper samples mounted in epoxy. In every

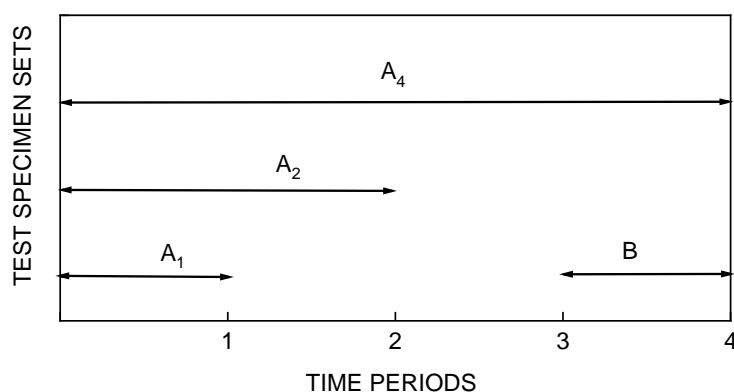


Figure 2. Principle of the interval test.

test there were three samples and three successive measurements for every sample. Every measurement point in LPR monitoring is thus average of nine individual measurements. The tests were performed from  $-30$  mV to  $+30$  mV vs. OCP using scan rate  $1 \text{ mV s}^{-1}$ . Corrosion current densities were determined using the curve fit application of the measurement software. The length of the LPR monitoring tests was up to 5 weeks. The Quartz Crystal Microbalance tests used copper deposited on 5 MHz AT-cut Cr/Au crystals. The tests were done by immersing the sample in test water and monitoring weight change at 10 second intervals. The length of the QCM tests was up to 5 days. QCM measurements were done with 2 to 4 replicates. LPR and QCM tests were done in 1-litre glass reactors at a gas purging rate of  $0.2 \text{ dm}^3 \text{ min}^{-1}$ . The groundwater was adapted from Olkiluoto final deposition site groundwaters [26] and pore water was adapted from [27]. The water compositions are shown in Table 1.

During the immersion tests the water properties were measured using a Hanna HI98194 Multiparameter Meter (Hanna Instruments, Smithfield, RI, USA). The meter measures temperature, pH, oxidation-reduction potential, dissolved oxygen, conductivity, and atmospheric pressure, and other water properties are calculated using these measurements. The important properties in this research were pH and dissolved oxygen that will affect passivation and electrochemical corrosion rate. Monitoring of pH and dissolved oxygen during the immersion tests are shown in Figures 3 and 4.

Table 1. Test water compositions.

Component	Ground water, mg/l	Pore water, mg/l
Na	3610	1000
Cl	5340	80
SO <sub>4</sub>	582	1300
Ca	279	4
Mg	102	4
K	87.5	12
Br	42	
HCO <sub>3</sub>	13.7	960
Sr	7.71	
Si	6.25	
B	1.38	
F	0.74	
Mn	0.168	
pH	7.9	10
TDS	10070	3360

## RESULTS

### Immersion tests

Immersion tests in ground water and pore water were done under air and nitrogen bubbling at room temperature. The aim was to provide corrosion rates to support life-time estimates of copper canister during the oxic period and during the period when the underground environment changes to oxygen deficient. The corrosion rates measured in air-purged ground water follow typical trends, Figure 5, and the sample sets are shown in chronological

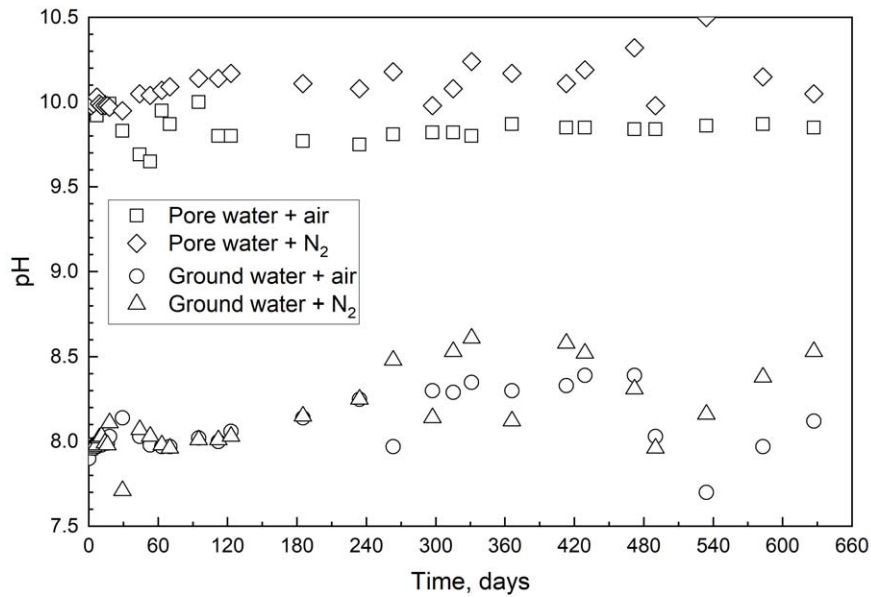


**Figure 3.** pH monitoring during the immersion tests.

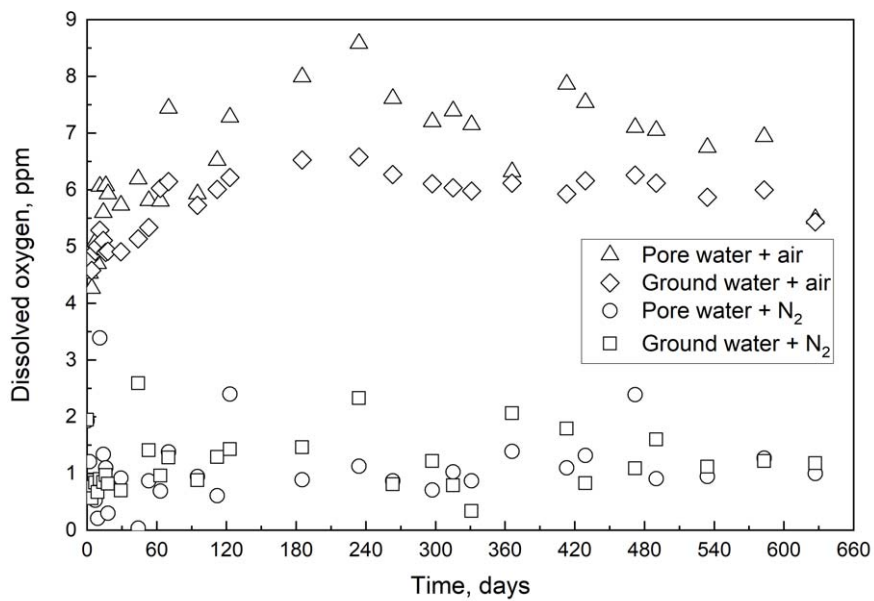


**Figure 4.** Dissolved oxygen monitoring during the immersion tests.

order. The corrosion rates decrease with time indicating formation of some protective corrosion products and corrosion rates of 2-month batches decrease with time indicating decrease in water corrosivity. The errors shown in Figure 5 are calculated by using standard deviation divided by square root of number of replicate samples (i.e. 5).

The air-purged ground water is the most corrosive of our test environments, and there the changes are clear. Also in other test environments similar trends were seen, Figure 6. Figure 6 shows the decreasing trend in corrosion rate with time. The data points in Figure 6 are calculated as averages of replicate experiments for 2, 4 and 8 months.

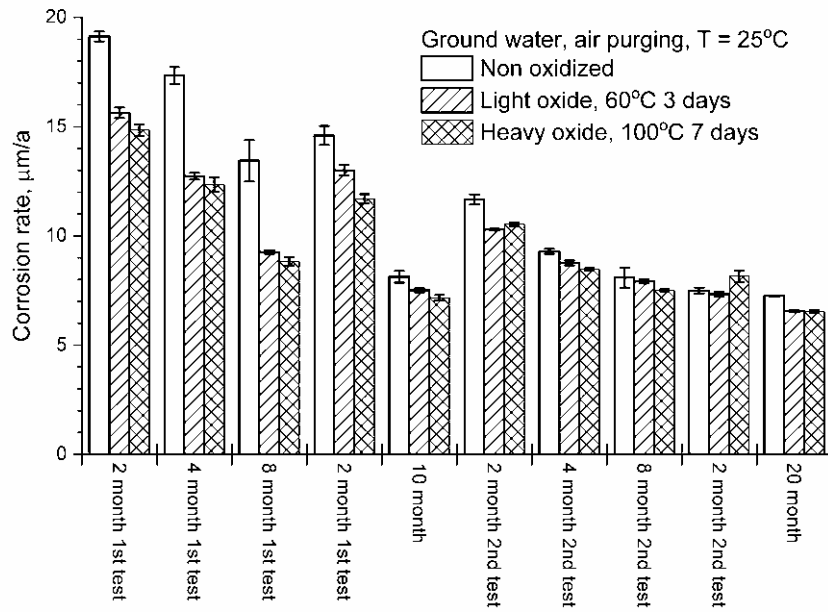


Figure 5. Average corrosion rates for five replicate immersion samples in air-purged ground water.

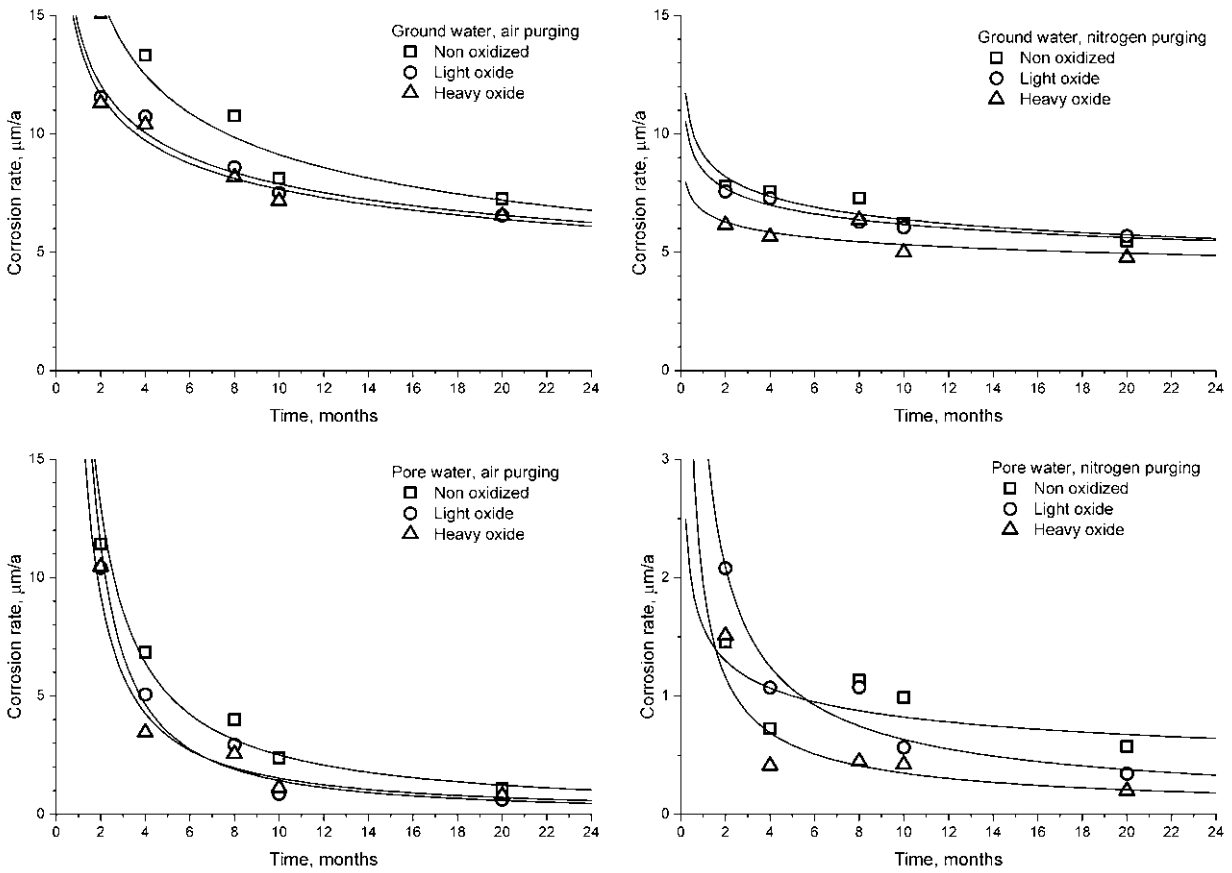


Figure 6. Decrease in corrosion rate with time in the immersion tests.

The corrosion rate in ground water purged with air approaches 6-8  $\mu\text{m}/\text{year}$  and when purged with nitrogen 5-7  $\mu\text{m}/\text{year}$ . The corrosion rate in pore water purged with air decreases to 1-2  $\mu\text{m}/\text{year}$  and when purged with nitrogen to less than one  $\mu\text{m}/\text{year}$ .

The corrosion rates were modelled using a power law equation. The model equations were of the form shown in equation (9),

$$r = A \cdot t^B \quad (9)$$

where  $r$  is corrosion rate in  $\mu\text{m}/\text{year}$  and  $t$  is time in months. The factors in equation (9) and their errors were determined by using a double logarithmic plot, equation (10)

$$\log(r) = \log(A) + B \cdot \log(t) \quad (10)$$

The model errors were estimated by calculating the minimum and maximum values given by factors  $A$  and  $B$ .

The calculated model equations measured in all environments are summarized in Table 2. The factor values show that the initial corrosion rate described by factor  $A$  is higher in air-purged than in nitrogen-purged systems. This is explained by the higher rate of the cathodic reaction and the concentration of dissolved oxygen. The initial corrosion rate in air-purged pore water is higher than in air-purged ground water. This can be explained by the lower concentration of dissolved salts in pore water

allowing higher oxygen solubility. The corrosion rate decreases faster in air-purged waters than in nitrogen-purged waters and this is shown by comparing the factor  $B$  values. Formation of a reaction product film requires a minimum concentration of copper ions on the surface before the compound formation becomes thermodynamically possible. In air-purged waters copper ions will form faster resulting in faster reaction product layer formation.

The effect of oxide films was done by comparison of the models by plotting the models as error band plots for up to 24 months' time. The plots in Figure 7 show that in air-purged ground water the oxide films produced in air provide some protection at the beginning of immersion. The differences in corrosion rates at longer exposure times are small. In other environments no differences were seen; also the error bands overlapped like in Figure 8 for nitrogen-purged ground water. It can be concluded that based on the immersion tests at room temperature the oxide films will not protect but neither increase corrosion rate after about few months.

#### Polarization resistance tests

In the polarization resistance monitoring tests only non-oxidized samples and samples with heavier oxidation at 100°C for 7 days were used. The polarization resistance monitoring results show that the corrosion current density decreases quite

**Table 2.** Models of immersion test corrosion rates for 2 to 20 month test lengths.

Water	Purging	Oxidation	Factor A	Factor B	R <sup>2</sup>
Ground	Air	None	20.073±1.12	-0.342±0.05	0.934
Ground	Air	60°C, 3 days	14.492±1.07	-0.264±0.03	0.949
Ground	Air	100°C, 7 days	13.945±1.07	-0.260±0.03	0.951
Ground	Nitrogen	None	9.126±1.09	-0.155±0.04	0.812
Ground	Nitrogen	60°C, 3 days	8.453±1.04	-0.136±0.02	0.952
Ground	Nitrogen	100°C, 7 days	6.750±1.12	-0.103±0.06	0.474
Pore	Air	None	26.318±1.23	-1.021±0.10	0.976
Pore	Air	60°C, 3 days	27.680±1.56	-1.288±0.22	0.973
Pore	Air	100°C, 7 days	19.911±1.38	-1.114±0.16	0.971
Pore	Nitrogen	None	1.581±1.43	-0.284±0.18	0.497
Pore	Nitrogen	60°C, 3 days	3.483±1.32	-0.741±0.14	0.922
Pore	Nitrogen	100°C, 7 days	1.942±1.51	-0.747±0.20	0.853

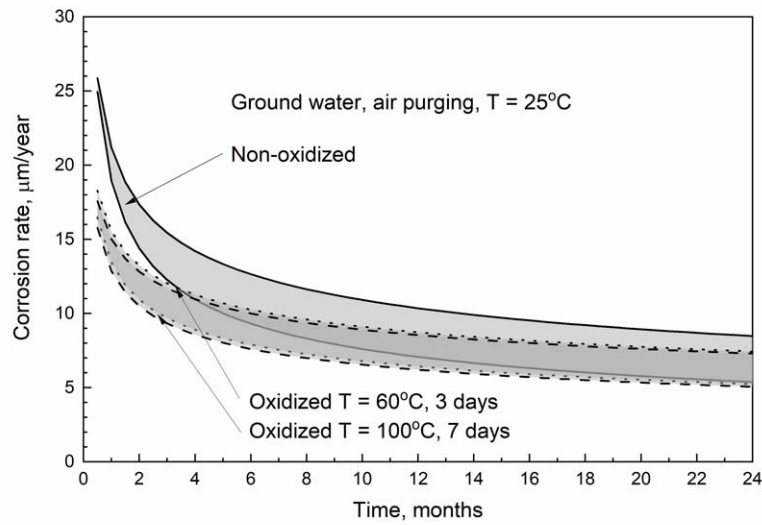


**Figure 7.** Comparison of corrosion rates in air-purged ground water.

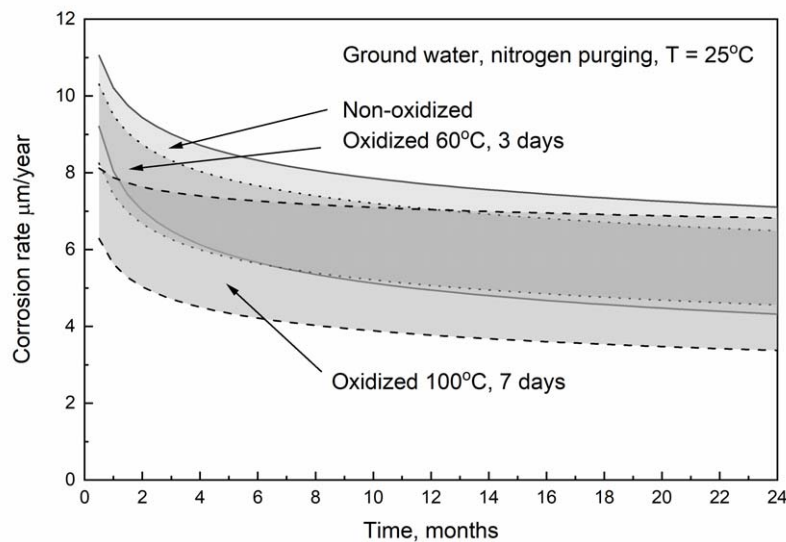


**Figure 8.** Comparison of corrosion rates in nitrogen-purged ground water.

rapidly with time and approaches a steady level within couple of weeks. Figure 9 shows an example of LPR measurements in ground water under nitrogen-purging and Figure 10 in pore water under air-purging. The steady-state corrosion rates in ground water under air-purging were 2-4  $\mu\text{m}/\text{year}$ , and corrosion rates of oxidized samples were about 1  $\mu\text{m}/\text{year}$  higher than those of non-oxidized samples. In nitrogen-purged ground waters corrosion rates of non-oxidized samples were 5-7  $\mu\text{m}/\text{year}$  and those of oxidized samples 2-4  $\mu\text{m}/\text{year}$ . The

steady-state corrosion rates in pore water under air-purging were less than 1  $\mu\text{m}/\text{year}$  both for oxidized and non-oxidized samples. In nitrogen-purged ground waters steady-state corrosion rates of non-oxidized samples were 1-2  $\mu\text{m}/\text{year}$  and those of oxidized samples 2-3  $\mu\text{m}/\text{year}$ . The errors in Figures 9 and 10 are calculated by using standard deviation divided by square root of number of replicate measurements (i.e. 9).

The corrosion rates were analysed using a power law equation (9) and its double logarithmic plot (10)

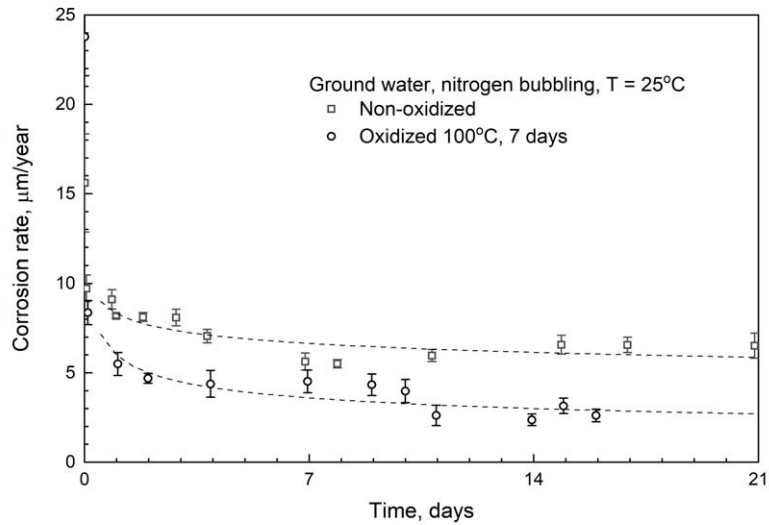


**Figure 9.** Corrosion rates measured in ground water under nitrogen-purging.

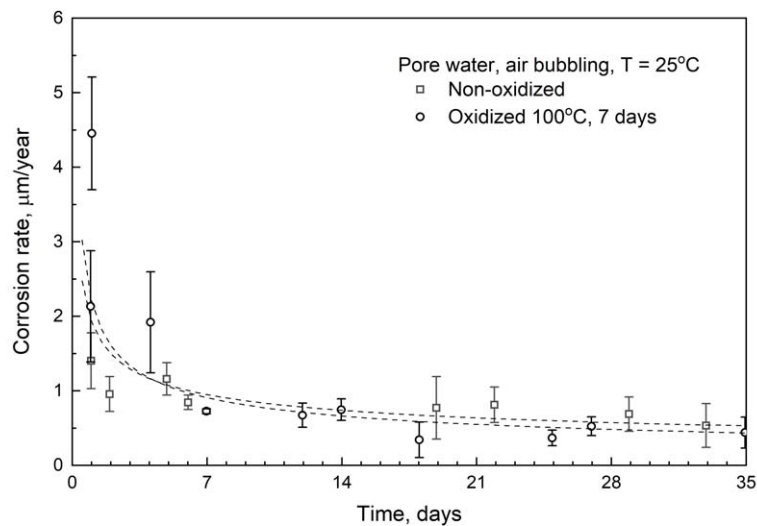


**Figure 10.** Corrosion rates measured in pore water under air-purging.

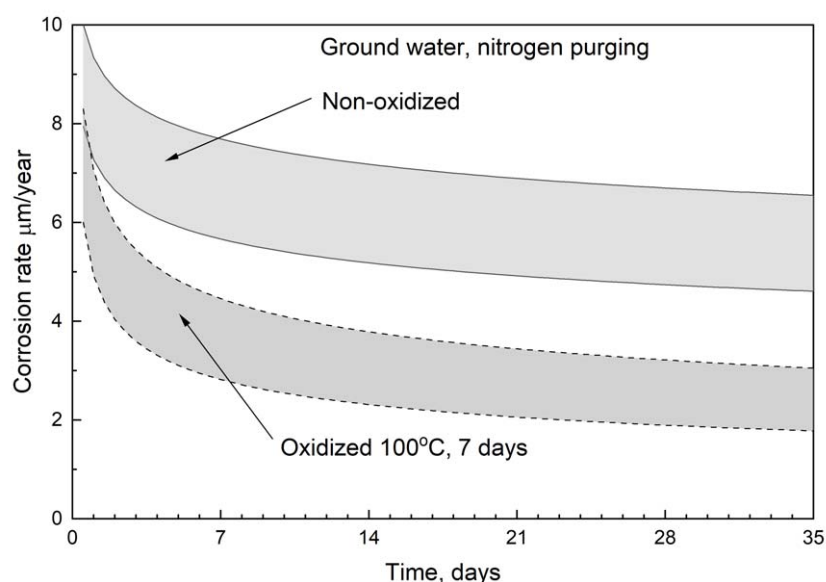
as in the weight loss measurements. The model equations are shown in Table 3, and the corrosion rates are in  $\mu\text{m}/\text{year}$  and  $t$  is time in days. The factor values do not always show same trends as the immersion test values in Table 2. The initial corrosion rate described by factor A can be higher or lower in air-purged than in nitrogen-purged systems. This factor is not a reliable indicator for the effect of the oxide film, as rapid changes in corrosion rate can happen in the first couple of days. The corrosion rate decreases usually faster in air-purged waters than in nitrogen-purged waters

and this is shown by comparing the factor B values. Formation of a reaction product film requires a minimum concentration of copper ions on the surface before the compound formation becomes thermodynamically possible. In air-purged waters copper ions will form faster resulting in faster reaction product layer formation.

Figures 11 and 12 show comparisons of corrosion rate models derived from LPR monitoring as error band plots. Under air-purging the corrosion rates did not differ in either ground water or pore water.

**Table 3.** Model equations of corrosion rate from LPR monitoring.

Water	Purging	Oxidation	Factor A	Factor B	R <sup>2</sup>
Ground	Air	None	4.346±1.05	-0.215±0.02	0.937
Ground	Air	100°C, 7 days	6.639±1.11	-0.277±0.05	0.904
Ground	Nitrogen	None	8.306±1.03	-0.114±0.01	0.852
Ground	Nitrogen	100°C, 7 days	5.980±1.06	-0.261±0.03	0.913
Pore	Air	None	1.926±1.11	-0.363±0.04	0.924
Pore	Air	100°C, 7 days	2.205±1.15	-0.456±0.05	0.882
Pore	Nitrogen	None	4.830±1.12	-0.568±0.05	0.931
Pore	Nitrogen	100°C, 7 days	3.438±1.05	-0.136±0.02	0.803

**Figure 11.** Comparison of corrosion rate models in nitrogen-purged ground water.

Under nitrogen-purging the corrosion rate was higher for non-oxidized copper than for oxidized in ground water (Figure 11), but in nitrogen-purged pore water the corrosion rate of oxidized samples was higher (Figure 12).

#### Quartz Crystal Microbalance tests

The short-term Quartz Crystal Microbalance tests showed that usually the weight decreases first rapidly and then weight change evens out. During the first 10-20 minutes the weight could even show some increase. In some cases, after active and continuous weight decrease, the weight began to increase again indicating formation of a reaction

product layer. The trends in QCM measurements were that in ground water the weight loss rate was much higher in air-purged than in nitrogen-purged water whereas in pore water the differences were small. Figure 13 shows that in ground water use of nitrogen-purging that results in dissolved oxygen level of 0.08-0.09 ppm effectively stops corrosion. The non-oxidized sample will even start to form a protective corrosion product layer. The air-purged water contains 8.3 ppm of dissolved oxygen. In air-purged water the non-oxidized sample develops a reaction product layer, but it will not protect, and the corrosion rate remains constant. Figure 14 shows weight change of non-oxidized and oxidized

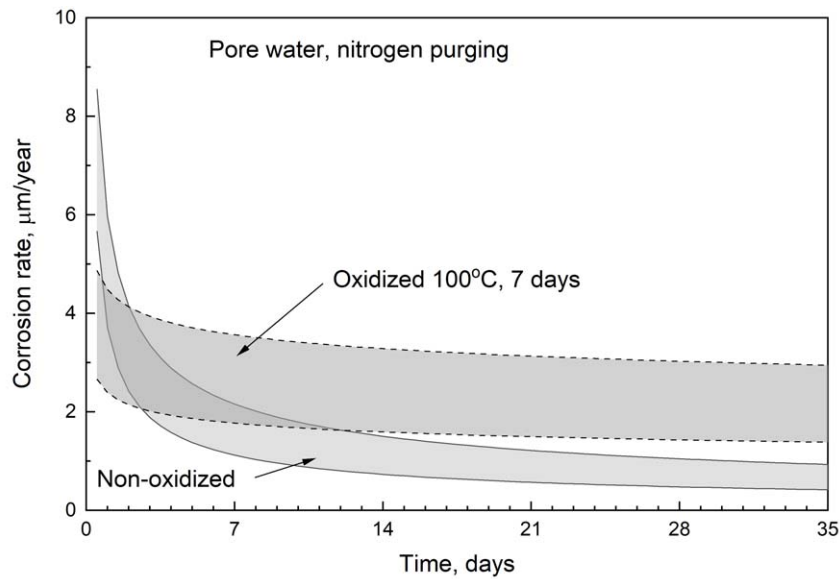


**Figure 12.** Comparison of corrosion rate models in nitrogen-purged pore water.

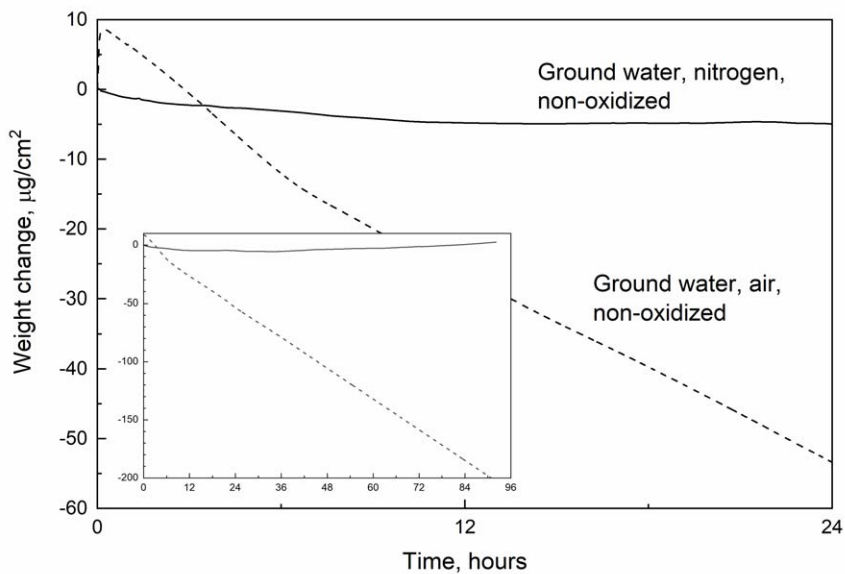


**Figure 13.** Weight change of QCM samples in air-purged and nitrogen-purged ground water.

sample in nitrogen-purged pore water. Both samples show weight decrease that evens out and turns to weight increase. The weight changes are very small due to low dissolved oxygen content and the high pH promotes passivation. Table 4 shows determined corrosion rates based on steady weight loss rates determined after the initial period lasting up to thousands of seconds. The corrosion rates show quite strong deviations, especially in ground

waters. The corrosion rates in ground waters are clearly higher than those determined by immersion tests or polarization resistance tests, whereas those determined in pore water are similar to other measurements.

## DISCUSSION

The corrosion rate of copper in waters depends on the oxidant concentration and formation of passive

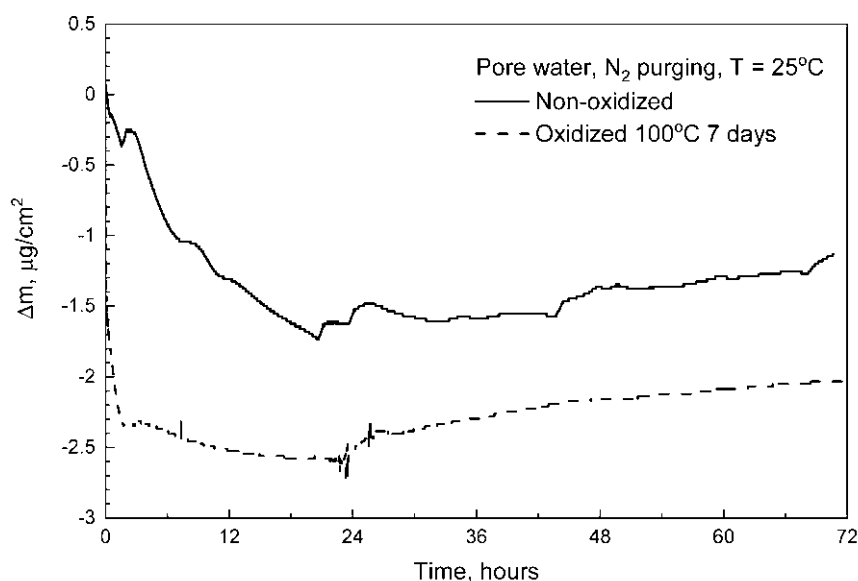


**Figure 14.** Corrosion rate based on weight change of oxidized and non-oxidized QCM samples in nitrogen-purged pore water.

**Table 4.** Corrosion rates determined from QCM measurements.

Water	Purging	Oxidation	r μm/a
Ground	Air	None	42.1±18.7
Ground	Air	100°C, 7 days	16.5±8.2
Ground	Nitrogen	None	14.0±7.4
Ground	Nitrogen	100°C, 7 days	8.8±4.9
Pore	Air	None	1.5±0.2
Pore	Air	100°C, 7 days	2.4±0.2
Pore	Nitrogen	None	0.8±0.2
Pore	Nitrogen	100°C, 7 days	0.3±0.1

films. In the test waters the oxidants are dissolved oxygen and cupric ion. The test waters were under constant purging of air or nitrogen. In the immersion tests the concentration of dissolved oxygen in air-purged waters was 6-7 ppm and in nitrogen-purged waters approximately 1 ppm. When comparing the immersion tests in air-purged and nitrogen-purged waters and assuming oxygen corrosion in a diffusion-controlled system, the corrosion rate in nitrogen-purged system should be approximately 15% of that in air-purged system. Using the models in Table 2 the ratio of calculated corrosion rates can be explained by dissolved oxygen in pore water for up to 4 months. With longer times the corrosion rate in

nitrogen-purged pore water was higher than what can be expected in a system with oxygen as the only oxidant. In ground water the corrosion rate in nitrogen-purged system was 50% of that in air-purged system at 2 months increasing to 80% at 20 months. This result shows that reduction of dissolved oxygen, reaction (1), is not the only cathodic reaction. Dissolved cupric species can be major oxidants as stated in [23].

The formation of the passive films depends on the concentration of copper ions near the surface, dissolved salts, and pH. The test waters in this research were synthetic ground water with pH = 8 and bentonite clay pore water with pH = 10.

Using the models derived from immersion tests (Table 2) the calculated corrosion rates in air-purged pore water are 80-95% of those in air-purged ground water at 2 months' time and decrease to 10-20% in 20 months. The corrosion rates in nitrogen-purged pore water are 15-30% of those in air-purged pore water at 2 months' time and decrease to 4-12% in 20 months. The immersion test results show clearly that the higher pH of pore water promotes passivation.

The corrosion rates in monitoring tests using linear polarization resistance measurements showed same decreasing trend as the long-term immersion tests. The corrosion rates reached a steady level after 1-2 weeks. Using the models shown in Table 3 the calculated corrosion rates from LPR measurements are 5% to 60% of those determined from immersion tests at 2 months' time. When extending the LPR models to 20 months' time the corrosion rates of LPR measurements are 15-25% of those measured by immersion tests. The exceptions are tests done in nitrogen-purged pore water with oxidized samples. These showed higher corrosion rates in LPR measurements than in immersion tests with long times.

The corrosion rates determined from QCM measurements were higher in ground water tests than with other measurement methods, but in pore water the corrosion rates were similar with other measurements. The errors were large in ground water tests but acceptable in pore water tests. The ground water tests show that corrosion rates under air-purging can be unexpectedly high. In ground water tests with nitrogen-purging high corrosion rates can be seen, but the copper surfaces do passivate. In pore water tests the samples passivate and corrosion rates remain low. In QCM tests similar trends were seen as with other measurements: Nitrogen-purging and high pH decrease corrosion rate and the oxide films have a small protective effect.

The main task of this study was to determine if the air-formed oxide films can promote or prevent general corrosion. Based on the immersion test models shown in Table 2, the oxide films can provide some protection. In ground water the oxidized samples show approximately 75% of the corrosion rate of non-oxidized samples after 2 months' time but after 20 months the corrosion rates of oxidized samples are approximately 90% of the non-oxidized. One exception is lightly

oxidized sample in nitrogen-purged ground water that shows corrosion rate of 94-98% of the non-oxidized sample over the whole time. In pore water the corrosion rates of oxidized samples were 70-90% of those of non-oxidized samples after 2 months' time. The corrosion rates of oxidized samples in pore water decreased to 30-60% of non-oxidized samples in 20 months. However, based on the error estimates, like shown in Figures 7 and 8 as error bands, we cannot show a definite protective effect by the oxide films. On the other hand, the results do show that the air-formed oxide films do not promote corrosion. The effect of oxide films in LPR tests was inconclusive. In air-purged ground water and pore water corrosion rates of non-oxidized and oxidized samples were similar. In nitrogen-purged ground water the corrosion rate of oxidized samples was lower than non-oxidized, but in nitrogen-purged pore water the corrosion rate of oxidized samples was higher. The results of QCM measurements show that the oxide films have a protective effect. In ground water the errors are so large that no solid conclusion can be made. In pore waters the errors are smaller, but in air-purged pore water oxide film increases corrosion and in nitrogen-purged pore water it decreases.

## CONCLUSIONS

Weight loss tests for up to 20 months showed that dissolved oxygen is not the only oxidant but dissolved cupric species can react in a cathodic reaction increasing copper corrosion rate. The corrosion rate in pH = 10 pore water is lower than in pH = 8 ground water and the copper passivates stronger in high-pH water with increasing immersion time. The corrosion rates based on the weight loss tests were 5-8  $\mu\text{m}/\text{year}$  in ground water and from less than one  $\mu\text{m}/\text{year}$  to 2  $\mu\text{m}/\text{year}$  in pore water. The concentration of dissolved oxygen affects the corrosion rate, but its effect is smaller than what is expected from the measured oxygen levels. The systems have also other compounds that can act as oxidants, such as cupric species.

The air-formed oxide films can provide a protective effect, but this effect is not very strong. At the beginning of the immersion tests the corrosion rates of oxidized samples were approximately 75% of the non-oxidized samples. The protective

effect decreased with time in ground water and after 20 months the oxidized samples showed corrosion rates that were 90% of the non-oxidized ones. In pore water the oxidized samples seemed to passivate stronger than the non-oxidized ones. After 20 months in pore water the oxidized samples showed corrosion rates that were 30-60% of non-oxidized ones. Short-term LPR and QCM measurements indicate that the corrosion rate decreases rapidly, and the copper surface can develop a protective film in 1-2 days. These films can still react over longer time periods. The protective effect of air-formed films cannot be stated as certain, as the error estimates show overlapping results. The possible negative effect of air-formed oxide films to increase corrosion can be ruled out.

### ACKNOWLEDGEMENTS

This research was funded by The Ministry of Economic Affairs and Employment financed project OXCOR (The effect of oxide layer on copper corrosion in repository conditions) in the Finnish Research Programme on Nuclear Waste Management (KYT2022). This study utilized the Academy of Finland's RawMatTERS Finland Infrastructure (RAMI) based jointly at Aalto University, GTK, and VTT in Espoo.

### CONFLICT OF INTEREST STATEMENT

The authors declare no conflict of interest. The funders had no role in the design of the study; in the collection, analyses, or interpretation of data; in the writing of the manuscript, or in the decision to publish the results.

### REFERENCES

1. Posiva Oy. 2017, Safety Case Plan for the Operating Licence Application., Report POSIVA 2017-02, Posiva Oy, Eurajoki, 152.
2. Posiva Oy and Svensk Kärnbränslehantering AB. 2017, Safety functions, performance targets and technical design requirements for a KBS-3V repository. Report POSIVA-SKB 2017-01, POSIVA Oy & SKB, 120.
3. Raiko, H., Pastina, B., Jalonen, T., Nolvi, L., Pitkänen, J. and Salonen, T. 2012, Canister Production Line 2012. Report POSIVA 2012-16, Posiva Oy, Eurajoki, 174.
4. King, F., Lilja, C., Pedersen, K., Pitkänen, P. and Vähänen, M. 2012, An Update of the State-of-the-art Report on the Corrosion of Copper Under Expected Conditions in a Deep Geologic Repository. Report POSIVA 2011-01, Posiva Oy, Eurajoki, 246.
5. Nolvi, L. 2009, Manufacture of Disposal Canisters. Report POSIVA 2009-03, Posiva Oy, Eurajoki, 76.
6. Pinnel, M. R., Tompkins, H. G. and Heath, D. E. 1979, *Appl. Surf. Sci.*, 2, 558-577.
7. Zhong, C., Jiang, Y., Luo, Y., Deng, B., Zhang, I. and Li, J. 2008, *Appl. Phys. A*, 90, 263.
8. Roy, S. K., Bose, S. K. and Sircar, S. C. 1991, *Oxid. Met.*, 35, 1.
9. Ramanandan, G. K. P., Ramakrishnan, G. and Planken, P. C. M. 2012, *J. Appl. Phys.*, 111, 123517.
10. Platzman, I., Brener, R., Haick, H. and Tannenbaum, R. 2008, *J. Phys. Chem. C*, 112, 1101.
11. Suzuki, S., Ishikawa, Y., Isshiki, M. and Waseda, Y. 1997, *Materials Transactions, JIM* 38, 1004.
12. Iijima, J., Lim, J-W., Hong, S-H., Suzuki, S., Mimura, K. and Isshiki, M. 2006, *Appl. Surf. Sci.*, 253, 2825.
13. Roy, S. K. and Sircar, S. C. 1981, *Oxid. Met.*, 15, 9.
14. Feng, Z., Marks, C. R. and Barkatt, A. 2003, *Oxid. Met.*, 60, 393.
15. Unutulmazsoy, Y., Cancellieri, C., Chiodi, M., Siol, S., Lin, L. and Jeurgens, L. P. H. 2020, *J. Appl. Phys.*, 127, 065101.
16. Derin, H. and Kantarli, K. 2002, *Appl. Phys. A*, 75, 391.
17. Zhu, Y., Mimura, K. and Isshiki, M. 2004, *Oxid. Met.*, 61, 293.
18. Wersin, P. 2013, LOT A2 test parcel, Compilation of copper data in the LOT A2 test parcel. SKB Technical Report TR-13-17, Swedish Nuclear Fuel and Waste Management Co, Stockholm, 28.
19. Rosborg, B., Kranjc, A., Kuhar, V. and Legat, A. 2011, *CEST*, 46, 148.
20. King, F., Lilja, C. and Vähänen, M. 2013, *J. Nuc. Mat.*, 438, 228.
21. Vazquez, M. V., de Sanchez, S. R., Calvo, E. J. and Schiffrin, D. J. 1994, *J. Electroanal. Chem.*, 374, 189.

- 
22. Vukmirovic, M. B., Vasiljevic, N., Dimitrov, N. and Sieradzki, K. 2003, *J. Electrochem. Soc.*, 150, B10.
  23. King, F., Kolar, M. And Maak, P. 2008, *J. Nuc. Mat.*, 379, 133.
  24. Kear, G., Barker, B. D. and Walsh, F. C. 2004, *Corr. Sci.*, 46, 109.
  25. McNeil, M. B. and Little, B. J. 1992, *J. Am. Inst. Cons.*, 31, 355.
  26. Huttunen-Saarivirta, E., Rajala, P. and Carpén, L. I. 2016, *El. Acta*, 203, 350.
  27. Vikman, M., Matuszewicz, M., Sohlberg, E., Miettinen, H., Järvinen, J., Itälä, A., Rajala, P., Raulio, M., Itävaara, M., Muurinen, A., Tiljander, M. and Olin, M. 2018, Long-term experiment with compacted bentonite. VTT Technology, Report No. 332. VTT Technical Research Centre of Finland, Espoo, 84.